Physica Scripta

PAPER

A high-performance NO_2 gas sensor based on silicon nanowire array

RECEIVED
17 April 2025

REVISED
22 August 2025

ACCEPTED FOR PUBLICATION
27 August 2025

PUBLISHED
10 September 2025

Zhenyu Jin[1], **Zhixiao Fang**[1], **Zai Wang**[1], **Wentao Wu**[1], **Dongfang Yan**[1], **Xun Yang**[2,*], **Yu Gao**[1], **Weihuang Yang**[1], **Dong Linxi**[1,*], **Gaofeng Wang**[1], **Xin Tong**[3], **Zhenhua Wu**[3,*], **Serguei Lazarouk**[4], **Vladimir Labunov**[4] **and Chaoran Liu**[1,*]

[1] Ministry of Education Engineering Research Center of Smart Microsensors and Microsystems, College of Electronics and Information, Hangzhou Dianzi University, Hangzhou 310018, People's Republic of China
[2] School of Electronic and Information Engineering, China West Normal University, Nanchong 637002, People's Republic of China
[3] Research Center for New Energy Technology, Shanghai Institute of Microsystem and Information Technology (SIMIT), Chinese Academy of Sciences (CAS), Shanghai 201800, People's Republic of China
[4] Faculty of Radioengineering and Electronics, Belarusian State University of Informatics and Radioelectronics, 220013 Minsk, Belarus
[*] Authors to whom any correspondence should be addressed.

E-mail: yangxun@cwnu.edu.cn, donglinxi@hdu.edu.cn, wuzhx@mail.sim.ac.cn and liucr@hdu.edu.cn

Keywords: NO_2 gas sensor, silicon nanowire array, high-specificity and sensitivity, portable

Abstract

Nitrogen dioxide (NO_2) gas detection is crucial for atmospheric environmental safety, industrial production monitoring, and traffic exhaust emission control. Reported detection devices often suffer from poor portability, insufficient selectivity, and demanding application requirements. Herein, we present a portable high-specificity and sensitivity NO_2 gas sensor based on silicon nanowire array field-effect transistors (SiNW FETs). The NO_2 gas sensor is fabricated on a (111) silicon-on-insulator (SOI) by the standard MEMS technology, which achieving high consistency in the dimensions of silicon nanowires. The experimental results demonstrated that the as-fabricated NO_2 gas sensor has a high sensitivity of 20 kΩ ppm^{-1} and a detectable minimum NO_2 concentration of 1.31 ppm. In addition, the NO_2 gas sensor exhibits a remarkable specificity, as evidenced by its significantly higher response to NO_2 compared to SO_2, CO, NH_3, O_3, C_2H_5OH and air. The developed portable sensor signal processing system achieves real-time monitoring and display of NO_2 concentration in the atmosphere. Furthermore, this research provides a high precision, easy installation and low cost NO_2 detector, indicating a good potential for industrial and civil applications in the future.

1. Introduction

NO_2 is one of the major gases emitted from industrial waste and automobile internal combustion engines, contributing to air pollution and health issues [1, 2]. The hazardous concentration limit for NO_2 exposure within one hour is 200 μg m^{-3} (0.106 ppm), with a warning threshold of 400 μg m^{-3} according to WHO clinical data. Acute exposure to NO_2 at parts-per-million (ppm) levels can induce adverse health effects, including respiratory irritation, ocular discomfort, and cephalalgia [1, 3, 4]. Consequently, the deployment of highly sensitive and portable NO_2 monitoring systems is imperative for the timely identification of atmospheric contamination and industrial leakages. Such proactive detection capabilities are critical for implementing effective mitigation strategies, thereby safeguarding public health and minimizing ancillary socioeconomic burdens associated with healthcare and environmental rehabilitation [5–7].

Numerous research institutions and enterprises are actively developing novel materials to enhance the sensitivity, selectivity, and stability of NO_2 gas sensors. Moreover, the global emphasis on environmental protection and the increase in market demand have provided strong support for the development of NO_2 gas detection technologies. However, several currently available mature NO_2 gas detection technologies all exhibit certain limitations. For example, the chemiluminescence method detects NO_2 by generating a light signal through a chemical reaction [8–10]. However, this technology is sensitive to environmental interference, which may lead to false positives. Another example is the spectroscopic method, analyzing the characteristic absorption NO_2 of peaks using ultraviolet or infrared spectroscopy. However, this technology is expensive and

© 2025 IOP Publishing Ltd. All rights, including for text and data mining, AI training, and similar technologies, are reserved.

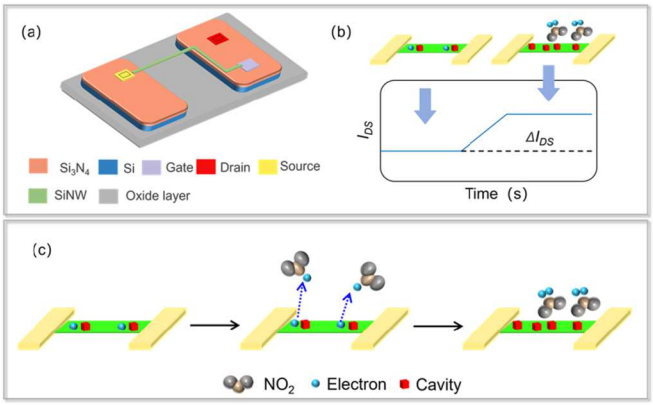

Figure 1. Structure and principle of the silicon nanowire array NO_2 gas sensor. (a) components of the silicon nanowire array NO_2 gas sensor (b) Working principle of NO_2 gas sensor (c) Mechanism diagram of NO_2 adsorption on the surface of the silicon nanowire array.

requires specialized operation and maintenance [11–13]. Most existing NO_2 gas monitoring sensors face significant challenges, including low selectivity, stringent environmental requirements, and poor portability. Therefore, realizing a NO_2 detection method that considers selectivity, portability and high sensitivity is of great significance for future industrial applications and scientific research [14, 15].

Silicon nanowire (SiNW) array field-effect transistors (FETs) have emerged as a compelling sensing element for biochemical detection systems, distinguished by their exceptional attributes [16]. These include a high surface-to-volume ratio that amplifies analyte interactions, inherent miniaturization potential that facilitates low-cost batch fabrication, and superior electronic properties that engender high signal-to-noise ratios and remarkable sensitivity. Furthermore, the functionalization flexibility of SiNW surfaces provides a pathway to achieving high selectivity toward target gases.

In this paper, we propose a NO_2 gas sensor system based on a silicon nanowire array field-effect transistor [17–19]. The nanowire structure has a higher aspect ratio and surface-to-volume ratio than thin films, resulting in excellent high-sensitivity performance. The silicon nanowire field-effect transistor array is a resistive element with a linear resistance change characteristic of 20 kΩ ppm^{-1}, providing good environmental adaptability for the system. The design of this system will address issues associated with existing NO_2 monitoring sensors such as complex installation, high costs, strict environmental requirements, and inconvenient portability.

2. System design

We fabricated a silicon nanowire array FET-based gas sensor system for real-time NO_2 concentration monitoring in ambient air [20, 21]. The system exhibits a sensitivity as high as 20 kΩ ppm^{-1}, enabling highly sensitive and accurate detection of NO_2 gas. The silicon nanowires array FET exhibits good linearity in the concentration range of 5 ppm to 20 ppm. The sensor can operate effectively at low concentrations, facilitating early detection of air quality issues or industrial safety hazards (e.g., NO_2 leaks), thereby mitigating NO_2-related environmental pollution and health risks. Additionally, the system is designed in a pen-like shape and compact. This design enables its widespread application in various scenarios, including industrial environments, indoor air quality monitoring and outdoor air quality monitoring.

The sensing mechanism hinges on the electron affinity of NO_2 molecules. Upon adsorption onto the SiNW surface, NO_2 acts as an electron acceptor, extracting electrons from the p-type SiNW channel. This surface charge transfer phenomenon depletes the majority hole carriers, thereby modulating the channel conductance. The resultant increase in source-drain current (I_{SD}) is quantitatively correlated with the ambient NO_2 concentration, providing the fundamental basis for detection [22] By measuring the change in resistance, the concentration of NO_2 in the gas can be inferred. The structure and reaction mechanism of the silicon nanowire device are shown in figure 1.

The silicon nanowire array FET is utilized as the sensing element to detect the NO_2 of concentration, because it is a resistive element characterized by a linear resistance change at 20 kΩ ppm^{-1}. The resistance signal is then converted into a voltage output using a Wheatstone bridge circuit. This output is processed through a filter and a buffer to produce a smooth curve, ensuring isolation between the preceding and following stages of the system. The voltage signal is submitted to the embedded microprocessor control system through a high-performance analog-to-digital converter (ADC). The microcontroller system uses a series of digital signal

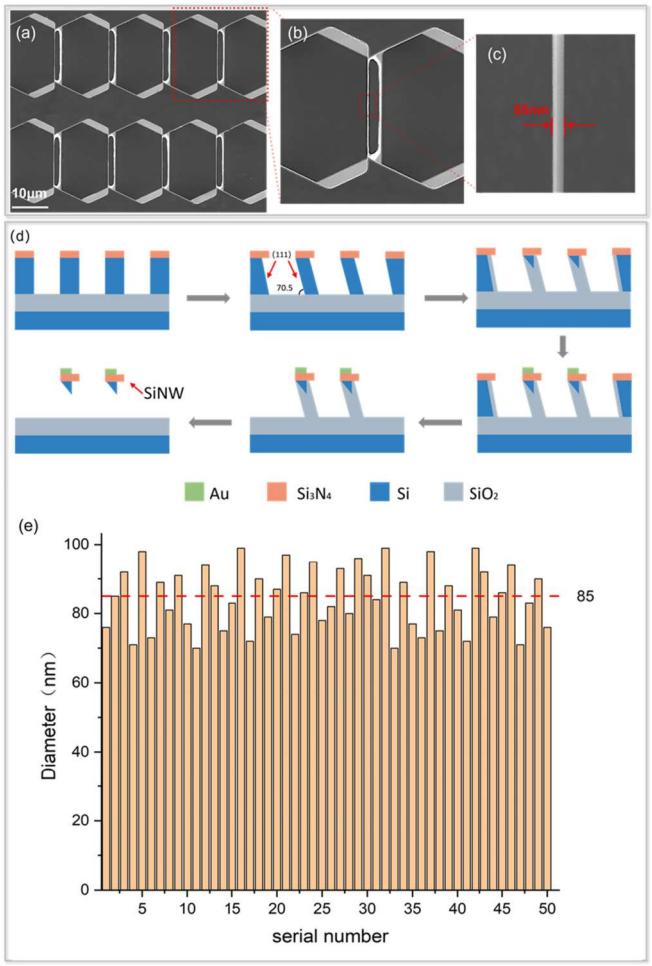

Figure 2. Preparation process of the silicon nanowire array NO_2 gas sensor. (a) The SEM image of SiNW array, the silicon nitride film of the device is removed to show its internal structure. (b) Local amplification diagram of the SiNW array. (c) SEM image of a single SiNW (d) Process for the preparation of silicon nanowire array. (e) Statistical chart of the diameter distribution for 50 silicon nanowire arrays.

processing algorithms to transmit the obtained data via the I^2C communication protocol, displaying the results on an OLED screen for visualization.

2.1. Preparation and structural analysis of the sensing element

The performance of the sensing element is crucial to the system. The silicon nanowire array NO_2 gas sensor is used to detect changes in NO_2 concentration in the air. The silicon nanowires exhibit a high degree of uniformity in diameter by the designed microfabrication processes for (111)-oriented SOI silicon wafers. Compared to single silicon nanowire devices, the detection signal capability of silicon nanowire array is stronger and more stable, with a significantly enhanced signal-to-noise ratio. This enables the detection of subtle variations in ambient NO_2 concentration and excellent dynamic response characteristics [16, 23].

First, the silicon wafer was anisotropically etched in a 40 wt% KOH solution at 50 °C to form hexagonal etch pits, with all sidewalls belonging to the (111) crystal plane family. Between two adjacent hexagonal pits, a single-crystal silicon thin-wall structure with a predefined width of 500 nm was formed. Next, a square window was etched in the silicon nitride layer at a specific region, followed by boron ion implantation and annealing. The ion implantation was performed at an energy of 40 KeV with a dose of $1E15cm^{-2}$, and the annealing was carried out at 1000 °C for 15 min. Subsequently, a gold electrode was fabricated in this region, while a gate electrode was patterned on the suspended silicon nitride thin film.

We achieve Triangular-cross-section SiNW arrays by precisely controlling the parameters of the wet etching process (wet etching time, wet etching rate, and dry etching depth). Additionally, a top gate electrode was designed to safeguard the SiNW from damage. Subsequently, following the establishment of electrode connections via ion implantation, the source and drain were fabricated, culminating in the packaging of the SiNW array field-effect transistors. The micrographs of the silicon nanowire array field-effect transistors and the fabrication flowchart are shown in figure 2.

The system employs a silicon nanowire array as the sensing element. Upon adsorption of NO_2 molecules on the silicon nanowire surface, electrons transfer from the nanowire to the unpaired orbitals of NO_2. This charge transfer increases the hole carrier density in the nanowire, thereby modulating the sensor's conductivity. A Wheatstone bridge circuit converts the resistance signal into a voltage output for MCU-compatible signal processing. The NO_2 concentration is quantified based on the calibrated voltage-concentration relationship.

2.2. Signal processing and detection system

The resistance change signal of the silicon nanowire array NO_2 gas sensor is not easily measurable directly by the microcontroller system. Therefore, signal conditioning through an analog circuit is necessary to convert the resistance signal into a measurable voltage signal.

The high sensitivity of the bridge means that even minor changes in resistance can be detected, and the Wheatstone bridge circuit can eliminate the effects of common-mode noise on the measurement results. Therefore, this can enhance the sensitivity of the NO_2 concentration detection system and improve the accuracy of the test results.

When the Wheatstone bridge is in an unbalanced state, the resistance of the silicon nanowire array can be calculated by using Kirchhoff's voltage law (KVL) and Kirchhoff's current law (KCL). From there, the concentration of NO_2 can be inferred.

Additionally, we designed a voltage follower circuit and a second-order Sallen-Key low-pass filter using the LM358 to achieve isolation between stages and remove high-frequency noise from the signal, thereby improving signal quality. The LM358 adopted is a widely used dual operational amplifier, compatible with a broad range of power supply voltages and commonly selected for implementing voltage followers and filters. The cutoff frequency of the low-pass filter can be calculated using the values of the resistors and capacitors. For the Sallen-Key low-pass filter, the formula for the −3dB cutoff frequency is:

$$f_c = \frac{1}{2\pi \cdot \sqrt{R_1 \cdot R_2 \cdot C_1 \cdot C_2}} \tag{1}$$

In equation (1), R_1 serves as the input-stage resistor, connecting the input signal to the operational amplifier's non-inverting input. R_2 functions as the feedback-stage resistor, linking the op-amp output to the capacitive node. C_1, bridging R_1 and R_2, creates the filter's first pole. C_2, connected between the op-amp's non-inverting input and ground, establishes the second pole. Substituting the values of the resistors and capacitors yields a −3dB cutoff frequency of 50 Hz, which can reduce power frequency interference.

The microcontroller system needs to collect, encode and transmit ADC signals to the serial port. Therefore, more ADC channels are required to enhance the ADC conversion accuracy and processing rate. To balance cost-effectiveness and performance, we selected the STM32F103C8T6. Its maximum clock frequency is 72 MHz and it is equipped with DMA (Direct Memory Access) functionality, which improves data transfer efficiency. Additionally, this MCU has two 18-channel 12-bit ADCs, capable of achieving a maximum sampling rate of approximately 1MSPS. The signal processing flow is displayed in figure 3(a).

The microcontroller system is powered by a 5 V battery. For power management, the HT7333 LDO (Low Dropout) linear regulator is adopted to step down the 5 V input to 3.3 V. It is a multifunctional LDO (Low Dropout). Its current output is 300 mA , the minimum standby current is only 2 μA and the output voltage accuracy is within ±2%. HT7333 helps to reduce the standby power consumption of the sensor system and improve the measurement accuracy. The PCB rendering and the structural diagram of the sensor system are shown in figures 3(b) and (c).

3. Results and discussion

3.1. The dynamic gas mixing test system

The gas sensitivity of NO_2 gas sensor is key to ensuring accurate measurements in the system. The experimental setup employs a dynamic gas mixing test system. The dynamic gas mixing method generates standardized gas streams by precisely blending a calibrated NO_2 source with a dilution gas at programmable flow ratios. The dilution ratio can be calculated based on the flow ratio of the two gas streams, allowing for the determination of the concentration of the standard gas. We control the gas flow via a computer and a high-precision mass flow controller (AB-700) to flexibly configure the desired concentration of target gas. The system mainly consists of three parts: the gas mixing system, the test circuit board and the data acquisition system [24–26].

The specific calculation formula for standard gas concentration is as follows:

$$\rho = \rho_0 \times q_{V_1}/(q_{V_2} + q_{V_1}) \tag{2}$$

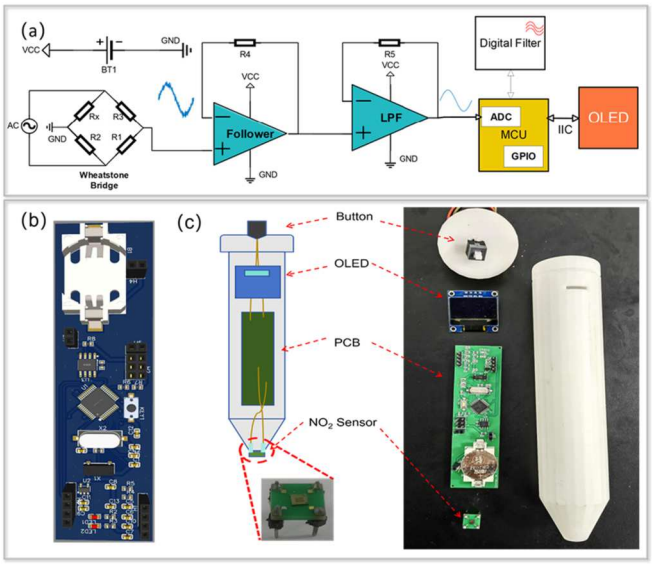

Figure 3. The process of how the system works. (a) Signal processing (b) PCB of the sensor system (c) Constitution of the sensor system.

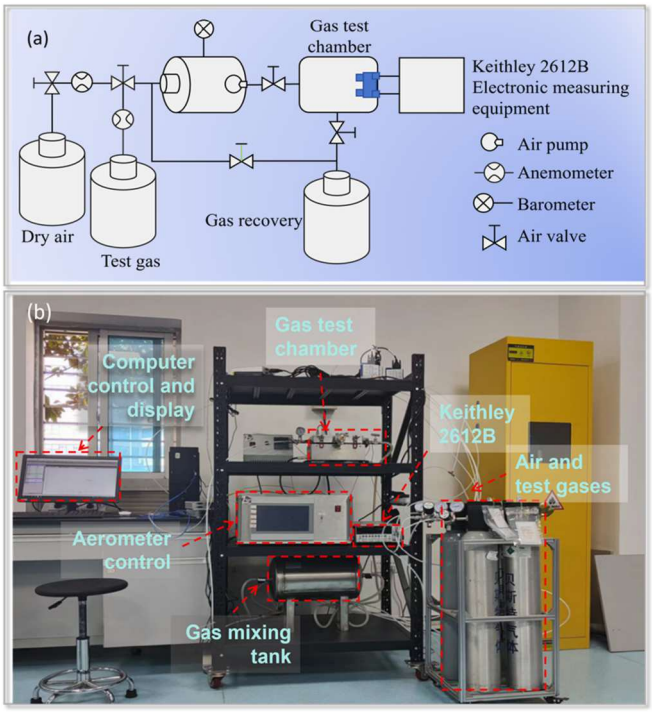

Figure 4. Test environment and system. (a) Schematic diagram (b) Real object.

In the formula: ρ, ρ_0—mass concentrations of the prepared standard gas and the test gas of a specific concentration (units: mg/m^3), qv_2, qv_1—flow rates of the dilution gas and the test gas (units: ml/min). We have constructed a dynamic testing system using silicon nanowire array devices to test different concentrations of NO_2. The model of the testing system shows in figure 4(a) and the physical diagram is shown in figure 4(b). The sensing element of the sensor system was connected to a sealed container via silver wires, while maintaining constant illumination, temperature, and humidity parameters. The concentration of test gas was controlled through the host computer of the dynamic gas mixing system. The gas is introduced into a sealed container after preparing a specific gas of concentration using the dynamic gas mixing device. Once stabilized, the resistance changes across the silicon nanowire device are recorded.

3.2. Signal processing and detection algorithm

The framework is established by configuring timers (to generate specific baud rates) and registers related to the ADC. When data is transmitted by the ADC, it is blocked due to waiting for register access. To optimize data throughput, a dual-buffer architecture is implemented with global interrupts, enabling continuous data acquisition while preventing access conflicts. Consequently, DMA is configured for the ADC to automatically transfer sensor data from the ADC register to buffer array 1, allowing the CPU to handle other tasks. Once the data transfer is complete, the contents of buffer array 1 are copied to buffer array 2 and DMA immediately begins the next data acquisition cycle. With the introduction of DMA, data transfer does not require CPU intervention, significantly reducing the CPU load.

In digital signal processing, this system employs a median average filtering algorithm. First, N samples are taken continuously, removing one maximum and one minimum value and then calculating the arithmetic average of the remaining N-2 samples. This algorithm effectively eliminates sampling value deviations caused by sporadic impulse interference. It also provides good suppression of periodic interference, resulting in a high smoothness of the generated voltage data curve.

Then, in the test environment, first measure the resistances of the silicon nanowire arrays corresponding to five concentrations, namely 5 ppm, 10 ppm, 15 ppm, and 20 ppm, to obtain a straight-line relating concentration to resistance. Then, through the formula of the Wheatstone bridge, inversely deduce that different ADC sampling values correspond to different NO_2 concentrations.

3.3. Sensor system sensitivity

As established in our previous work [27], the SiNW devices exhibit distinct humidity response characteristics. Considering this established humidity sensitivity, all NO_2 sensing measurements in the current study were conducted under strictly controlled humidity conditions to eliminate environmental interference.

In the dynamic testing system, the gas under test is in a flowing state, which requires a longer time to reach equilibrium. As shown in figure 5(a), it can be observed that the resistance of SiNW decreases with the increase in the concentration of the target gas, exhibiting good linearity in the range of 0–20 ppm. In the repeatability experiment of figure 5(b), it can be observed that the response time of SiNW is 156 s, the recovery time is 251 s, and the repeatability is good.

3.4. Sensor selectivity

The test results and selectivity coefficients during the stable response period, processed by MATLAB filtering, for NO_2, SO_2, CO, air, NH_3, O_3, and ethanol are shown in figure 5(c). The resistance changes during the test were compared with the concentration of the target NO_2 gas to evaluate the response of the gas to the sensing element. As shown in figure 5(c), the response value to NO_2 gas is significantly higher than that of other tested gases.

The essence of the sensor detecting NO_2 is the migration of electrons. Upon NO_2 adsorption on SiNW surfaces, two new transmission peaks emerge near the Fermi level (EF), indicating the introduction of new electronic states. These states likely originate from coupling between the LUMO of NO_2 and the conduction band of SiNWs, thereby enhancing electron transport. Acting as a strong electron acceptor, NO_2 extracts electrons from the SiNW surface, increasing hole concentration (p-type doping effect). The presence of unstable single electrons in NO_2 gas molecules facilitates the migration of electrons from the silicon nanowires to the gas molecules. This charge transfer significantly modifies the conductive properties of SiNWs, consequently reducing their resistance. In contrast, since the central atoms of SO_2 and CO possess no unpaired electrons, these gas molecules can only undergo physical adsorption on the silicon nanowire array. This results in a lower probability of electron transfer and consequently smaller resistance variations in the silicon nanowire array. Thus, this sensor exhibits good gas selectivity.

In summary, the sensor demonstrates high sensitivity exclusively towards NO_2 gas, with significantly lower responses to SO_2, CO, NH_3, O_3, C_2H_5OH and air [28].

3.5. Data processing algorithms

The resistance curve lacks sufficient smoothness. This is due to the existence of high-frequency noise interference in the collected voltage signals. Therefore, this system employs an FIR digital low-pass filter to remove high-frequency noise spikes, achieving a smooth voltage curve. Since FIR filters are based on finite impulse response, they are always stable and do not exhibit instability due to feedback. Additionally, they offer high design flexibility, allowing adjustments to frequency response by selecting different window functions and filter orders, which is beneficial for future system upgrades.

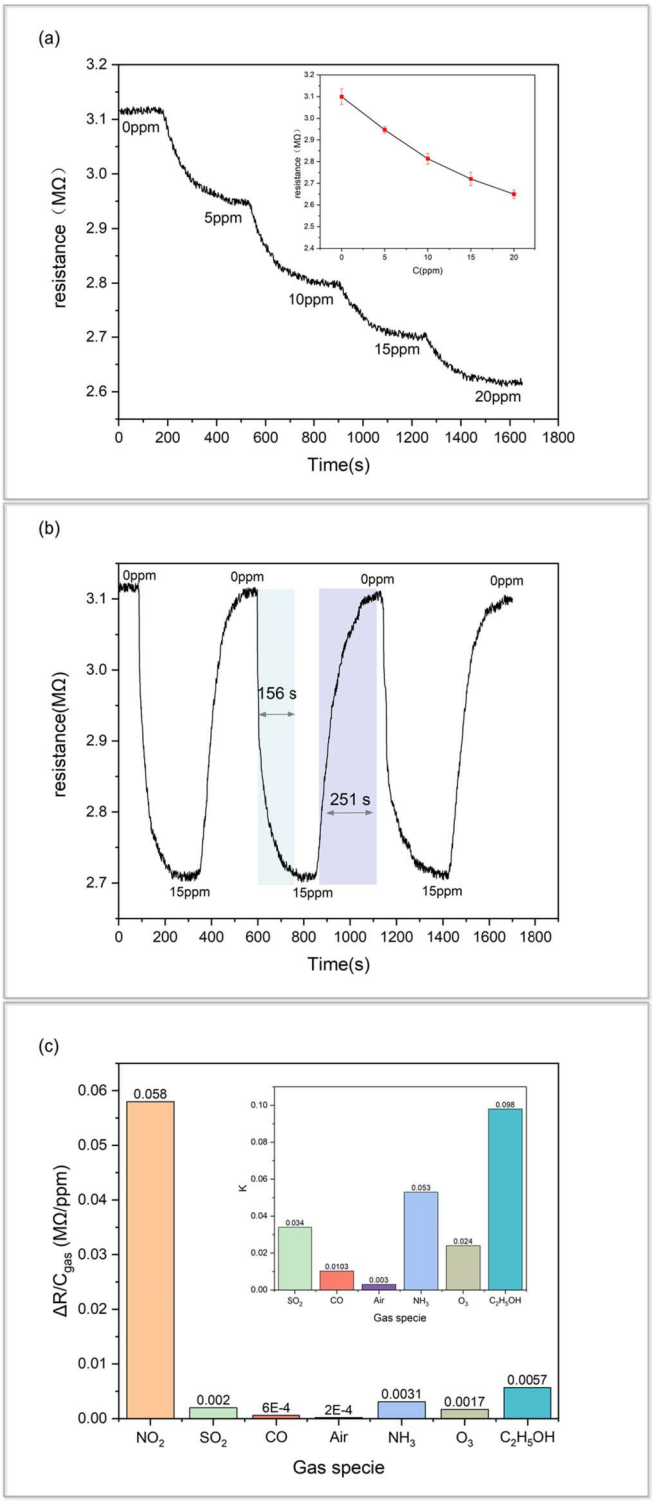

Figure 5. Gas selectivity and output performance testing. (a) Dynamic response of SiNW to NO_2 with different concentrations and linear transformation of resistance corresponding to NO_2 with different concentrations (b) Experimental results on the repeatability of SiNW arrays (c) Gas selectivity test results and selectivity coefficients.

3.6. Visualization of sensor system

This system uses a 0.96-inch OLED screen to display the measurement results, which is based on the comprehensive consideration of cost and display effect. Each pixel of the OLED screen is an individual light-emitting diode, which does not require backlighting like an LCD, making the OLED screen more energy-efficient. Additionally, OLED has a higher refresh rate and faster bus timing, which helps avoid blocking our program.

The OLED screen used in this system has four pins: power, ground, SDA (Serial Data) for data transmission, and SCL (Serial Clock Line) to control the timing of data transmission. This screen uses the I^2C communication protocol for data transfer.

The I^2C bus in this system has two types of signals during data transmission: the start signal and the stop signal. Start signal: When SCL is high, SDA transitions from high to low, indicating that the system starts transmitting data. Stop signal: When SCL is high, SDA transitions from low to high, indicating that the system ends the data transmission.

3.7. System test results

The silicon nanowire array NO_2 gas sensor of the system was placed in a dynamic gas mixing test system to measure different concentrations of NO_2, with the data displayed on the OLED screen recorded. As shown in figure 5, when the NO_2 concentration was as low as 5 ppm, the system was still able to accurately measure the NO_2 concentration in the air. The minimum detection limit is calculated to be 1.31 ppm using 3σ method, the sensor demonstrated excellent sensitivity.

4. Conclusion

In this study, we have developed a portable, highly sensitive and highly specific sensor system, which demonstrates high precision and reliability in monitoring and measuring the concentration of NO_2. Numerous experiments, including gas selectivity tests of the sensor, detection tests with varying NO_2 concentrations, and monitoring of NO_2 concentrations in the air near factories, have validated the system's ability to maintain consistency under different conditions.

This system exhibits high sensitivity (20 kΩ ppm^{-1}) and excellent selectivity, enabling rapid and accurate detection of NO_2 gas. The high sensitivity of this system demonstrates its great potential in environmental detection and helps people discover air quality problems or industrial safety hazards in advance.

Additionally, through optimizing manufacturing processes and establishing a network of NO_2 gas monitoring sensors, the system has significantly reduced costs, demonstrating great potential for widespread adoption.

Future work will focus on enhancing sensor accuracy, reducing response/recovery times, and further improving the system's dynamic response capability. Successfully integrating this system into practical applications in the industrial and agricultural sectors will provide new solutions for these fields, thereby advancing related scientific research and technological applications.

Acknowledgments

This work was supported in part by the National Key R&D Program of China (No. 2022YFB3204800) and the Fundamental Research Funds for the Provincial Universities of Zhejiang (No. GK249909299001-003).

Data availability statement

All data that support the findings of this study are included within the article (and any supplementary files).

References

[1] Kim Y *et al* 2019 Two-dimensional NbS_2 gas sensors for selective and reversible NO_2 detection at room temperature *ACS Sens.* **4** 2395–402
[2] Hoa L T, Tien H N, Luan V H, Chung J S and Hur S H 2013 Fabrication of a novel 2D-graphene/2D-NiO nanosheet-based hybrid nanostructure and its use in highly sensitive NO_2 sensors *Sensors Actuators B* **185** 701–5
[3] Vijjapu M T, Surya S G, Yuvaraja S, Zhang X, Alshareef H N and Salama K N J A S 2020 Fully integrated indium gallium zinc oxide NO_2 gas detector *ACS Sens.* **5** 984–93
[4] Tsai M F, Liao W C, Hsueh T J and Hsueh 2024 Comparative study of the sensitivity of H_2S and NO_2 in $CuInSe_2$ gas sensors that are fabricated using screen printing and MEMS Integration *Appl. Surf. Sci.* **676** 9
[5] Shen Y B, Zhong X X, Zhang J, Li T T, Zhao S K, Cui B Y, Wei D Z, Zhang Y H and Wei K F 2019 In-situ growth of mesoporous In_2O_3 nanorod arrays on a porous ceramic substrate for ppb-level NO_2 detection at room temperature *Appl. Surf. Sci.* **498** 10
[6] Wu Z L, Li Z J, Li H, Sun M X, Han S B, Cai C, Shen W Z and Fu Y Q 2019 Ultrafast response/recovery and high selectivity of the H_2S gas sensor based on α-Fe_2O_3 nano-ellipsoids from one-step hydrothermal synthesis *ACS Appl. Mater. Interfaces* **11** 12761–9
[7] Han Y T *et al* 2019 Interface engineered WS_2/ZnS heterostructures for sensitive and reversible NO_2 room temperature sensing *Sensors and Actuators B-Chemical* **296** 9
[8] Kim Y-S, Hwang I-S, Kim S-J, Lee C-Y and Lee J-H 2008 CuO nanowire gas sensors for air quality control in automotive cabin *Sensors Actuators B* **135** 298–303

[9] Nagarjuna Y and Hsiao Y-J 2024 TeO_2 doped ZnO nanostructure for the enhanced NO_2 gas sensing on MEMS sensor device *Sensors and Actuators B-Chemical* **401** 134891
[10] Tamaki J, Miyaji A, Makinodan J, Ogura S and Konishi S 2005 Effect of micro-gap electrode on detection of dilute NO_2 using WO_3 thin film microsensors *Sensors and Actuators B-Chemical* **108** 202–6
[11] Hu H, Yang X, Guo X, Khaliji K, Biswas S R, Garcia de Abajo F J, Low T, Sun Z, Dai Q and Dai 2019 Gas identification with graphene plasmons *Nat. Commun.* **10** 1131
[12] Zhang D, Luo N, Xue Z, Bai Y and Xu J 2024 Hierarchically porous ZnO derived from zeolitic imidazolate frameworks for high-sensitive MEMS NO_2 sensor *Talanta* **274** 125995
[13] Wang Y, Liu C Y, Wang Z, Song Z W, Zhou X Y, Han N and Chen Y F 2019 Sputtered SnO_2:NiO thin films on self-assembled Au nanoparticle arrays for MEMS compatible NO_2 gas sensors *Sensors and Actuators B-Chemical* **278** 28–38
[14] Premkumar V K, Vishnuraj R, Sheena T S, Yang X, Pullithadathil B, Zhang C and Wu Z J J o A 2024 Compounds, Influence of ZnO hexagonal pyramid nanostructures for highly sensitive and selective NO2 gas sensor *J. Alloys Compd.* **994** 174625
[15] Zhao X, Xu Z, Zhang Z, Liu J, Yan X, Zhu Y, Attfield J P and Yang M J N C 2025 Titanium nitride sensor for selective NO2 detection *Nat. Commun.* **16** 182
[16] Li D, Chen H, Fan K, Labunov V, Lazarouk S, Yue X, Liu C, Yang X, Dong L and Wang G 2021 A supersensitive silicon nanowire array biosensor for quantitating tumor marker ctDNA *Biosens. Bioelectron.* **181** 113147
[17] Guo M, Brewster Ii J T, Zhang H, Zhao Y and Zhao Y 2022 Challenges and opportunities of chemiresistors based on microelectromechanical systems for chemical olfaction *Acs Nano* **16** 17778–801
[18] Rai P, Raj S, Ko K-J, Park K-K and Yu Y Y-T 2013 Synthesis of flower-like ZnO microstructures for gas sensor applications *Sensors and Actuators B-Chemical* **178** 107–12
[19] Chen X W, Wang S, Su C, Han Y T, Zou C, Zeng M, Hu N T, Su Y J, Zhou Z H and Yang Z 2020 Two-dimensional Cd-doped porous Co_3O_4 nanosheets for enhanced room-temperature NO_2 sensing performance *Sensors and Actuators B-Chemical* **305** 10
[20] Wong W S, Raychaudhuri S, Lujan R, Sambandan S, Street R A and Street 2011 Hybrid Si nanowire/amorphous silicon FETs for large-area image sensor arrays *Nano Lett.* **11** 2214–8
[21] Li Y, Liu C, Zou H, Che L, Sun P, Yan J, Liu W, Xu Z, Yang W and Dong L J C R P S 2023 Integrated wearable smart sensor system for real-time multi-parameter respiration health monitoring *Cell Reports Physical Science* **4** 101191
[22] Hu K, Cai Y, Wang Z, Zhang Z, Xian J and Zhang C 2024 A review on metal oxide semiconductor-based chemo-resistive ethylene sensors for agricultural applications *Chemosensors* **12** 13
[23] Halpern J M, Wang B and Haick H 2015 Controlling the sensing properties of silicon nanowires via the bonds nearest to the silicon nanowire surface *ACS Appl. Mater. Interfaces* **7** 11315–21
[24] Zhang W, Yuan R, Chai Y Q, Zhang Y and Chen S H 2012 A simple strategy based on lanthanum-multiwalled carbon nanotube nanocomposites for simultaneous determination of ascorbic acid, dopamine, uric acid and nitrite *Sensors and Actuators B-Chemical* **166** 601–7
[25] Kumar U, Yang Y H, Deng Z Y, Lee M W, Huang W M and Wu C H 2022 *In situ* growth of ternary metal sulfide based quantum dots to detect dual gas at extremely low levels with theoretical investigations *Sensors and Actuators B-Chemical* **353** 131192
[26] Gupta S, Knoepfel A, Zou H, Ding Y J S and Chemical A B 2023 Investigations of methane gas sensor based on biasing operation of n-ZnO nanorods/p-Si assembled diode and Pd functionalized Schottky junctions *Sensors and Actuators B-Chemical* **392** 134030
[27] Yang X, Zheng C, Liu J, Yu J, Long L, Xu Z, Dong L, Yao D and Liu C J P S 2024 High-precision silicon nanowire array sensor for quantitating ambient humidity and pH value *Phys. Scr.* **99** 035968
[28] Zou H, Guo L, Xue H, Zhang Y, Shen X, Liu X, Wang P, He X, Dai G and Jiang P J N C 2020 Quantifying and understanding the triboelectric series of inorganic non-metallic materials *Nat. Commun.* **11** 2093